J Membrane Biol (2015) 248:991–1004
DOI 10.1007/s00232-015-9810-0

Identification and Partial Characterization of Two Populations of Prostasomes by a Combination of Dynamic Light Scattering and Proteomic Analysis

Davide Chiasserini[1] · Michela Mazzoni[2] · Federico Bordi[4,5] · Simona Sennato[6] · Federica Susta[3] · Pier Luigi Orvietani[3] · Luciano Binaglia[3] · Carlo Alberto Palmerini[2]

Received: 9 March 2015 / Accepted: 19 May 2015 / Published online: 12 June 2015

Abstract Prostasomes are vesicles secreted by prostate epithelial cells and are found in abundance in the semen. Here we characterized two different prostasome populations isolated from human seminal fluid. Prostasomes were isolated using differential centrifugation, while dynamic light scattering (DLS) was used to characterize their size and size distribution. Their protein content was analyzed using two-dimensional electrophoresis and mass spectrometry. DLS showed two distinct prostasome subpopulations in centrifuged seminal plasma, with an average hydrodynamic radius of 80 and 300 nm. The larger population was isolated after centrifugation at 20,000 × *g* (P20), while the smaller one was recovered at 100,000 × *g* (P100). The two fractions had a similar lipid composition, showing an elevated content of sphingomyelin and cholesterol. The P100 vesicles showed a significant over-expression of proteins involved in the endosomal sorting complexes required for transport (ESCRT) machinery such as Alix, TSG101, and syntenin-1. Some proteins possibly involved in prostate cancer were present only in one specific population (TMPRSS2 in P100 and VCP in P20). The different size and protein profile in the two subpopulations of prostasomes might support differential roles of the semen vesicles toward the target cells, and/or different secretion pathways from the organ of origin.

Keywords Prostasome · Seminal vesicle · Proteomics · Dynamic light scattering · Exosomes

Davide Chiasserini and Michela Mazzoni have contributed equally to the work.

Electronic supplementary material The online version of this article (doi:10.1007/s00232-015-9810-0) contains supplementary material, which is available to authorized users.

✉ Carlo Alberto Palmerini
carlo.palmerini@unipg.it

[1] Sezione di Neurologia, Dipartimento di Medicina, Università degli Studi di Perugia, Perugia, Italy

[2] Dipartimento di Scienze Agrarie, Alimentari ed Ambientali, Unità di Ricerca di Biochimica e Biologia Molecolare, Via del Giochetto, 06125 Perugia, Italy

[3] Sez di Fisiologia e Biochimica, Dipartimento di Medicina Sperimentale, Università degli Studi di Perugia, Perugia, Italy

[4] Dipartimento di Fisica and CNR-IPCF, Sapienza Università di Roma, piazzale A. Moro, 2, 00185 Rome, Italy

[5] Center for Life Nano Science@Sapienza, Istituto Italiano di Tecnologia, Viale Regina Elena, 291, 00161 Rome, Italy

[6] ISC-CNR, UOS Sapienza, P.le Aldo Moro 2, 00185 Rome, Italy

Introduction

Human seminal fluid contains mature spermatozoa, and it is composed by the secretions of several glands. Among these, there are the testes, the prostate, the seminal vesicles, and other minor accessory glands (Mann and Lutwak-Mann 1981). The seminal plasma, that is the semen devoid of spermatozoa, carries out several different functions. As an example, we mention the coagulation/liquefaction of semen after ejaculation and the buffering properties that may help neutralize the acidic milieu of the vagina (Mann and Lutwak-Mann 1981). Biochemical composition of seminal plasma has been thoroughly studied (for a review see Juyena and Stelletta 2012). In the late seventies of the last century, Ronquist identified in human seminal fluid a vesicular component called prostasomes (Arvidson et al. 1989; Fabiani 1994; Ronquist and Frithz 1986). More recently, it became clear that semen contains a variety of membranous extracellular vesicles (EV). Among these,

prostasomes are derived from prostatic epithelial cells (Ronquist 1987; Rooney et al. 1993). Other tissues within the male genital tract may contribute to the secretion of EVs into seminal plasma. For example, epididymosomes (Wilson et al. 1984) are derived from epididymal epithelial cells, and other vesicles are further provided by the vesicular glands and by the vasa deferentia (Lilja and Weiber 1983; Wilson et al. 1984). However, while it would be certainly more appropriate to use the term prostasome for the vesicles produced by the prostatic epithelium only (Olsson and Ronquist 1990), this term is often applied to the whole variety of membrane vesicles isolated from seminal plasma (Stegmayr and Ronquist 1982). The lipid composition of these vesicles is peculiar; cholesterol is present in high amounts as is sphingomyelin, whereas phosphatidylcholine is less abundant (Arienti et al. 1998; Arvidson et al. 1989). Prostasomes are also rich in Ca^{2+}, GDP, ADP, and ATP (Fabiani 1994; Ronquist and Frithz 1986), and many proteins of their surface possess catalytic activity (Fabiani 1994) or are involved in the immune response (Rooney et al. 1993). Protein content of seminal plasma has been investigated both with classical biochemical techniques and with high-throughput methods such as proteomics. Several classes of proteins are present in seminal prostasomes, including ATPases, kinases, transferases, lipases, and glycolytic enzimes (Lilja and Weiber 1983; Olsson and Ronquist 1990; Ronquist 1987; Wilson et al. 1984).

The physiological role of prostasomes is still not completely understood. In general, they are credited with the function of carrying information from prostate acinar cells to the mobile spermatozoa (Kelly 1995). They also appear to contribute to other functions such as the enhancement of sperm motility (Stegmayr and Ronquist 1982) the liquefaction of semen (Lilja and Laurell 1984), and immunosuppression (Kelly 1995; Kelly et al. 1991).

The exact molecular mechanisms at the basis of these complex functions are still not known; however, it is unlikely that these different tasks are accomplished by a single type of vesicle. In fact, also the properly-termed prostasomes, i.e., the prostasomes released by the prostate acinar epithelial cells, are rather heterogeneous both in size and appearance (Ronquist et al. 2012), showing a size distribution that ranges from 30 to 200 nm. Different subpopulations of prostasomes have been already isolated, showing different sizes and morphologies when studied at the electron microscope, and different protein and lipid composition (Aalberts et al. 2012; Brouwers et al. 2013).

While their extremely high resolution makes the sizing methods based on differential sedimentation very attractive, yet they are subject to several experimental artifacts, since the sedimentation rate depends on both the particles shape and density. Moreover, in the case of lipid vesicles, the density is affected not only by the composition as expected (Greenwood et al. 2006) but also by the size (Goormaghtigh and Scarborough 1986). Furthermore, the value of the estimated particle size with electron microscopy images can be affected by systematic errors, due both to the different steps employed in sample preparation (staining and sample drying) and to the relatively poor statistics, since only a comparatively small number of particles can be usually visualized. Dynamic light scattering (DLS) (Berne and Pecora 1976) thanks to the ability to investigate the particles in their "natural" environment, i.e., directly in the suspension, and to the excellent statistical framework, ideally complements microscopy, and separation techniques (Haridas and Bellare 1998).

In this study, different subpopulations of prostasomes isolated from human seminal fluid using differential centrifugation were characterized in terms of size and size distribution by DLS methods. The content of lipids and the aminopeptidase activity of the two populations of prostasomes were also compared. The global protein content was analyzed with a classical proteomic approach, i.e., two-dimensional electrophoresis (2-DE) for orthogonal polypeptide separation and liquid chromatography/tandem mass spectrometry (LC–MS/MS) for the identification of differential expressed polypeptides.

Materials and Methods

Reagents

Sephadex G-200, Urea, thiourea, CHAPS, SDS, and Tris-hydroxymethyl-aminomethane were obtained from GE Healthcare (Milano, Italy). Immobilized pH gradient strips (IPG strips, 17 cm; non-linear pH gradient 3–10), biolyte carrier ampholytes, bromophenol-blue, acrylamide, *N*,*N*′-methylenebisacrylamide, Bradford reagent, and Sypro Ruby stain were purchased from Bio-Rad (Milano, Italy). Benchmark Protein Ladder molecular weight standards (range 10–200 kDa) were obtained from Invitrogen (Milano, Italy). *N*-succinyl-ala-ala-ala-*p*-nitroanilide (Suc $(Ala)_3$pNA), *p*-nitroaniline, benzamidine hydrochloride, iodoacetamide, protease inhibitor cocktail, proteomic-grade trypsin, LC–MS-grade ACN, and all other chemicals were from Sigma-Aldrich (Milano, Italy).

Prostasome Isolation

All the procedures involving human subjects were performed according to the declaration of Helsinki and the internal guidelines of our university. All the semen samples were donated by healthy volunteers for whom informed consent was obtained. Semen prostasomes were obtained from fresh human semen, as previously described (Fabiani

1994). For the initial experiments, a pool of five semen samples (20–25 ml) from healthy volunteers between 20- and 30-year old was constructed. Briefly, seminal fluid was left for 30 min at room temperature to liquefy and then centrifuged at 800×*g* for 10 min and then 20 min at 10,000×g, to eliminate spermatozoa and cell debris. The supernatant was subsequently centrifuged at 100,000×*g* for 120 min and the pellet, containing prostasomes and amorphous material, was suspended in 2 mL 30 mM Tris, 130 mM NaCl, pH 7.4. Prostasomes were separated from amorphous material by gel filtration on a Sephadex G-200 column (1.5 × 30 cm) and eluted with 30 mM Tris, 130 mM NaCl (adjusted to pH 7.6 with HCl). Prostasomes were not retained by the column and were collected with V_0. The vesicles were finally harvested by centrifugation at 100,000×*g* for 120 min and suspended in 2 mL 30 mM Tris, 130 mM NaCl, adjusted to pH 7.4, and called "purified prostasomes" (PP).

The prostasomes isolated from single donors were centrifuged at 800×*g* for 10 min and then 20 min at 10,000×*g*. The supernatant was subsequently centrifuged at 100,000×*g* for 120 min and the pellet was suspended in 2 mL 30 mM Tris, 130 mM NaCl, pH 7.4. Aliquots of the PP fraction isolated from pooled and single donors were then analyzed by means of DLS.

Dynamic Light-Scattering Measurements

Size and size distribution of prostasomes were determined by DLS measurements carried out with a Brookhaven BI9000AT logarithmic correlator (Brookhaven Instr. Corp., Long Island, NY) at 25 °C. In this fiber-optic probe, the Gaussian laser beam transmitted by a monomode optical fiber illuminates the scattering volume, and a second monomode fiber, positioned at a fixed angle of 137.5°, collects the scattered light. Temperature was controlled within ±0.2 °C with a peltier system. To obtain the size distributions of semen prostasomes, the measured autocorrelation functions were analyzed using the cumulants method to obtain the average values of the particles size and exponential sampling algorithm to obtain the shape of the size distributions (Stepanek 1993). Details of the methods are reported elsewhere (Bordi et al. 2001).

Analysis of Phospholipid Classes

The extraction of lipid from membranes was performed as previously described (Folch et al. 1957). The chloroform phase was dried under a gentle stream of nitrogen and dissolved in known amounts of chloroform: methanol (2:1, v:v). Phospholipids were separated by two dimensional thin-layer chromatography (6.5 × 6.5 cm, PE SIL G250 m; Whatman Ltd., Maidstone, UK) with (a) chloroform:methanol:1.6 M ammonia (70:30:5, v:v) and (b) chloroform:acetone:acetic acid:methanol:water (75:30:15:15:7.5, v:v). Spots were visualized by exposure to I_2 vapors and identified with pure reference standards. After the sublimation of I_2, spots were scraped off the plate and their phosphorus content was determined as described by Bartlett (Bartlett 1959). All the determinations were performed on samples frozen at −80 °C.

Determination of Cholesterol

Free cholesterol was isolated by chromatography on silica gel 60-250 TLC (0.25 mm) sheets (Panreac, Barcelona, Spain), by using a solution of *n*-hexane/ethyl ether/acetic acid (40:10:1, v/v) as developing solvent. Plates were air-dried and immersed in a staining solution of 0.03 % Brilliant blue R in 20 % methanol (v/v) for 30 min (Nakamura and Handa 1984). Plates were then destained with 20 % methanol for 10 min and successively air-dried for 15 min; chromatograms were then elaborated electronically using a computer connected to a scanning apparatus. Data were processed with Image J, and quantitative assessment was achieved by comparison with reference standards.

Aminopeptidase Activity

We tested the aminopeptidase activity of semen prostasomes using Suc(Ala)3pNA as a substrate (Lilja and Laurell 1984). The incubation mixture contained, 4 mM Suc(Ala) pNA and 0.23 mM Tris–Cl buffer (pH 7.5) in a final volume of 0.7 ml. The reaction was started by adding 30 µl of prostasome (about 0.025 mg protein) and continued for 60 min at 25 °C. The absorbance at 410 nm was monitored continuously with a spectrophotometer Cary 3E. The activity was usually expressed in µmol hydrolyzed substrate × h^{-1} × mg^{-1} proteins.

Two-Dimensional Gel Electrophoresis (2-DE)

2-DE was performed as previously described (Chiasserini et al. 2011; Susta et al. 2010). Each protein sample (0.5 mL of the purified fractions) was precipitated overnight at −20 °C with cold acetone (1:4 v/v). The pellet was then washed once with cold acetone and solubilized with a buffer composed of Urea 7 M, Thiourea 2 M, CHAPS 2 %, Triton X-100 1 %, and 50 mM DTT.

Aliquots containing 0.1 mg of protein were diluted to 0.35 mL with same buffer by adding 0.2 % carrier biolyte ampholytes and trace amount of bromophenol blue in lysis buffer. IPG strips (17 cm, non-linear pH gradient 3–10) were rehydrated 1 h at 20 °C with the same diluted protein solutions. Hydratation was completed by applying a 50 V potential difference for additional 7 h at 16 °C in a Protean IEF Cell apparatus (Bio-Rad). Isoelectric focusing was performed at

16 °C in the same Protean IEF Cell apparatus by applying the following voltage/time profile: (i) 300 V for 3 h; (ii) 1 h linear voltage gradient from 300 to 3500 V; (iii) 3500 V for 3 h; (iv) 1 h linear voltage gradient from 3500 to 9500 V; and (v) 9500 V for 8 h up to a total of 85,000 Vh.

After isoelectric focusing, IPG strips were equilibrated for 15 min in a solution containing 6 M urea, 2 % SDS, 0.375 M Tris–HCl, pH 8.8, 20 % glycerol, and 130 mM DTT. Subsequently, strips were transferred to a second equilibration solution containing 6 M urea, 2 % SDS, 0.375 M Tris–HCl, pH 8.8, 20 % glycerol, 135 mM Iodoacetamide, and traces of bromophenol blue. After 10 min equilibration, strips were washed 5 min with SDS-PAGE running buffer, placed on the top of 10 %T polyacrylamide gels (200 × 200 × mm) and embedded in 1 % agarose stacking gel. SDS-PAGE separation was performed at 10 °C, by using an Ettan DALT six apparatus (GE healthcare, Amersham). After SDS-PAGE separation, proteins were fixed 0.5 h in 30 % methanol/10 % acetic acid and stained overnight with Sypro Ruby stain. Excess dye was washed out from the gel with an aqueous solution containing 30 % methanol and 10 % acetic acid. Stained polypeptide maps were digitally recorded by a Versadoc 1000 instrument (Bio-Rad).

An estimate of molecular weight and isoelectric point (pI) of isolated polypeptides was obtained, respectively, by running standard protein markers in a separate lane and from the spot position in the isoelectrofocusing coordinate.

Analysis of 2-DE Images

Digital gel images were analyzed using the PDQuest software (version 8.0, Bio-Rad, Hercules, CA, USA). After filtering gel images, spot detection and quantification were performed in both automatic and manual modes. Well-resolved spots appearing in all the gels were fixed as landmarks before comparing images in a match set. Non expression-related differences in spot intensity were corrected using the PDQuest "total quantity in valid spots" normalization mode. Only spots whose staining intensity was significantly different in the three experimental groups and exhibiting a fold change minimum of two were considered for MS identification. Statistical evaluation of PDQuest-normalized spot intensity values was performed using the SPSS version 16.0 software. Normality of spots distribution was evaluated using Shapiro–Wilk test ($p < 0.05$). As the results highlighted a non-parametric distribution of spot intensities, data were log2 transformed and analyzed with T test ($p < 0.05$).

Polypeptide Identification and Bioinformatics Analyses

In-gel digestion of isolated proteins was performed according to a previously described procedure (Susta et al. 2010). Heavily stained spots from two or three gels were analyzed separately, whereas faint spots from the five replicated gels of the same group were pooled for analysis. Oligopeptides were separated by a ProteomeX apparatus (Thermo Scientific, San Jose, CA, USA) equipped with a 100 µL loop, one Hypersil-Keystone BioBasic C18 capillary columns (0.18 × 100 mm), and configured in the Protein ID mode. The oligopeptide mixtures were injected in the RP-column equilibrated with 0.1 % formic acid (solvent A) and separated with a gradient of ACN containing 0.1 % formic acid (solvent B), at a flow rate of 2 µL/min. After in column injection, oligopeptides were eluted with a 35-min linear gradient from 5 % to 60 % solvent B, followed by a 5-min linear gradient from 60 % to 80 % solvent B and 8-min isocratic elution with 80 % solvent B. Columns were equilibrated 20 min with solvent A before loading next sample.

Eluted oligopeptides were electrosprayed directly into the LCQ Deca-XP^{Plus} ion-trap mass spectrometer. The electrospray source parameters were 12 units of sheath gas flow and 3.2 kV. Ion transfer capillary voltage and temperature were +18 V and 160 °C, respectively. Survey scan MS range was set at m/z 200–2000. Relative collision energy for collision-induced dissociation was set at 35 %. Each MS/MS spectrum was obtained by averaging three micro-scans with maximum injection time of 200 ms. MS/MS spectra were acquired in data-depending mode. Dynamic exclusion was enabled with a repeat count of two, a repeat duration of 0.5 min, and a 3-min exclusion duration window. All spectra were acquired in centroid mode. Database searching was performed by the MASCOT software version 2.2 (http://www.matrixscience.com/). Search parameters were as follows: protein sequence database Swiss-Prot release 2013_1 (43,688 sequences); enzyme trypsin; fixed modification carbamidomethylation; variable modification oxidation; two missed cleavages permitted; peptide tolerance ±1.2 Da; and MS/MS tolerance 0.6 Da, peptide charge +1, +2, and +3. MS output files with .dta extension were merged and converted in MASCOT generic format (MGF), using the Perl script available from the MASCOT website. Finally, the identification files were uploaded into the server. Spots recognized by LC–MS/MS data as a mixture of different polypeptides were identified as the hit with the highest MASCOT score ($p < 0.05$), on condition that this value was at least three times higher than that attributed to other proteins identified. Gene ontology (GO) and pathway analysis were performed with WEbGEstalt server (Wang et al. 2013), using GO slim ontologies. Analysis of the presence of signal peptides for secretion was made with the SecretomeP server (v. 2.0) (Bendtsen et al. 2004).

Results

Dynamic Light Scattering (DLS) of Semen Prostasomes

First, we applied DLS on prostasomes isolated from pooled seminal fluid samples ($n = 5$) to verify the size and size distribution of the vesicles. A typical distribution of the hydrodynamic radius of the prostasomes obtained from DLS measurements is shown in Fig. 1a. Two populations, one of the smaller particles, with a radius centered at $\approx$80 nm and a second one with radius peaked at $\approx$300 nm were present in all samples analyzed. Figure 1b shows the hydrodynamic diameter, <2R>, of the prostasomes as a function of the pH of the suspending medium, in the presence or absence of albumin. These values of the particles size were obtained from the cumulant analysis of the measured DLS correlation functions, hence representing an average over the whole size distribution. The average size of the prostasomes showed a significant decrease as the pH was increased from pH 5 to pH 7–8. Apparently, albumin did not modify this trend, although in the presence of albumin, the particles appeared systematically larger (about 10 %) at all the pH values investigated. This effect was probably due to the increased viscosity of the media where the prostasomes are suspended, due to the dissolved albumin. Since the hydrodynamic radius R was calculated from the measured diffusion coefficient D through the Stokes–Einstein equation, an increase of the medium viscosity reflects a proportional apparent increase of R. In

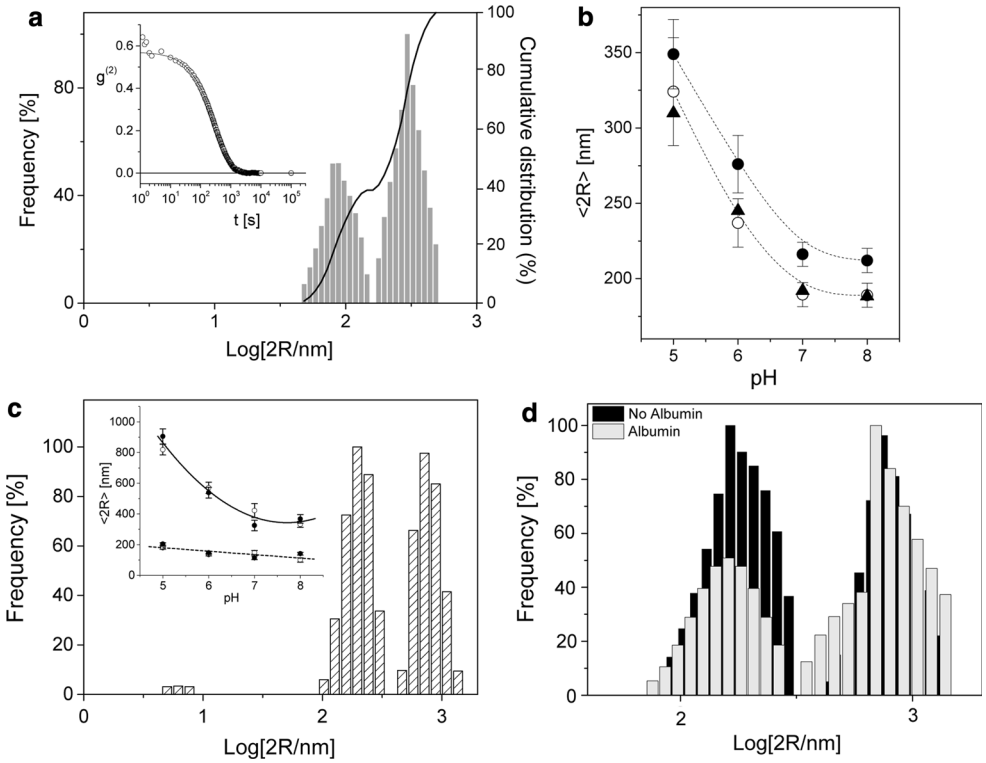

Fig. 1 Characterization of prostasome population in semen by DLS. **a** Typical distribution of the hydrodynamic radii of prostasomes obtained from DLS measurements. *Columns* represent the relative percentage of particles with a given diameter (2R in nm) on a Log scale. The continue curve represents the cumulative frequency distribution. Two populations, one of the smaller particles, with a radius centered at $\approx$80 nm and a second ones with radius peaked at $\approx$300 nm clearly appear. The *inset* shows the intensity–intensity correlation function of scattered light and the fitted curve from which the size distribution is extracted. **b** Average hydrodynamic diameter (from cumulant analysis) <2R> of the prostasomes as a function of the pH of the suspending medium, in the presence (*filled circles*) or absence (*empty circles*) of albumin. The lines are a guide to the eye only. As the pH is increased from pH 5 to pH 7–8, a significant decrease of the average size of the suspended particles is observed. Albumin does not modify this trend, however, for all the values of pH investigated, in the presence of albumin, due to the increased viscosity of the suspending medium, the particles appear larger. When the effect of the viscosity is taken into account (*filled triangles*) the radius of prostasomes in the presence or in the absence of albumin becomes much more similar. **c** Size distribution function of prostasomes at pH 5 in the presence of albumin. The small peak centered at about 6.5 nm is the protein dissolved in the medium. The inset shows the behavior of the average diameter of the two prostasome subpopulation as a function of pH, both in the presence (*empty symbols*) and in the absence (*filled symbols*) of albumin. Lines are a guide to the eye only. **d** Typical prostasomes' size distributions in the presence (*right slanted*) and in the absence (*left slanted*) of albumin. In this example, pH = 5.0

fact, the viscosity of an aqueous solution of BSA at a concentration of 40 mg/ml and at a temperature of T = 25 °C is ≈1.1 10^{-3} Pa s (Monkos 1996; Yadav et al. 2011), significantly higher than the viscosity of water in the same conditions, which is ≈0.91 10^{-3} Pa s (Monkos 1996; Yadav et al. 2011). When the effect of the viscosity was taken into account (Fig. 2b, filled triangles), the radius of prostasomes in the presence or in the absence of albumin became much more similar. Noteworthy, the albumin concentration value that gives the best matching of the values of the radii, corrected for the viscosity increase and in the absence of the protein, was 30 mg/ml, which is lower than the nominal concentration (40 mg/ml). This finding suggests that while part of the protein is dissolved in the suspending medium, a significant fraction (about 25 %) is adsorbed on the prostasomes and does not contribute to the viscosity increase. Figure 1c shows the typical result obtained when the correlation functions are analyzed in terms of size distributions: two distinct subpopulations clearly appeared, both in the absence and in the presence of albumin. In the latter case (as in this example), the free protein was also clearly distinguishable, with a radius of the order of ≈6.5 nm, which is consistent with the literature data (Jin et al. 2006; Vilker et al. 1979).

While the smaller population seemed to be rather insensitive to the pH variation, the size of the larger one decreased from ≈850 nm at pH 5 to ≈350 nm at pH 8.

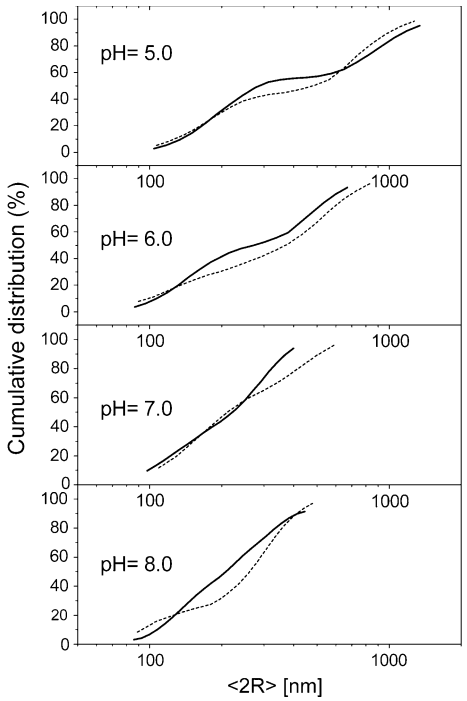

Fig. 2 Cumulative size distributions of semen prostasomes in the presence (*dashed lines*) and in the absence (*solid lines*) of albumin at different pH values

The presence of the albumin did not affect these values. However, if the total areas under the two peaks are considered, the weight in the distribution of the larger population increased in the presence of albumin. In Fig. 1d, two typical size distributions (in this example, pH = 5.0) in the presence and in the absence of albumin are compared. It is apparent that while the position of the peaks was not influenced by the presence of the protein, their relative area changed significantly and was almost inverted. The effect was even more evident when the cumulative distributions were compared.

In Fig. 2, the cumulative size distributions of prostasomes with and without albumin are compared at the four pH values investigated. Each curve was obtained as the average of six distinct samples. Although the average procedure tended to smooth the curves' features, the cumulative frequency of no-albumin samples grew more rapidly than the samples with albumin at all the different pH values investigated (with the possible exception of pH = 7.0). Next, we sought to investigate if the average size of the isolated prostasomes was depending from the donor age. We arbitrarily divided the donors in two groups, "young donors" (age ≤35 years, $n = 5$) and "elder donors" (age >35 years, $n = 5$), and studied the correlation between size and age using both the cumulant method and the exponential sampling method. In Fig. 3, the prostasomes average size is plotted as a function of the single donors' age. In the upper panel (Fig. 3a), the size is obtained by analyzing the measured correlation function with the cumulant method that does not distinguish different subpopulations, giving only an average value. In the two lower panels the size values are calculated using the exponential sampling algorithm, that is able to separate the two populations of prostasomes (Fig. 3b vesicles with radius ≈80 nm, Fig. 3c vesicles ≈300 nm). A weighted linear fit over the whole age interval suggested a linear dependence of the prostasome's size on the donor's age, both for the average size (cumulant analysis) and for the two subpopulations (exponential sampling). However, due to the low number of samples, the linear dependence could not be unequivocally demonstrated, even after data aggregation (Fig. 3d).

Separation of the Two Prostasome Populations

The measurement of prostasomes size distribution in human semen showed two different vesicle populations. To separate these two prostasome types from the PP fraction, we modified the protocol for differential centrifugation as shown in Fig. 4.

The PP fraction was resuspended in the Tris buffer and centrifuged at 20,000×g for 60 min. The supernatant was then centrifuged at 100,000×g for 120 min. Pellets were

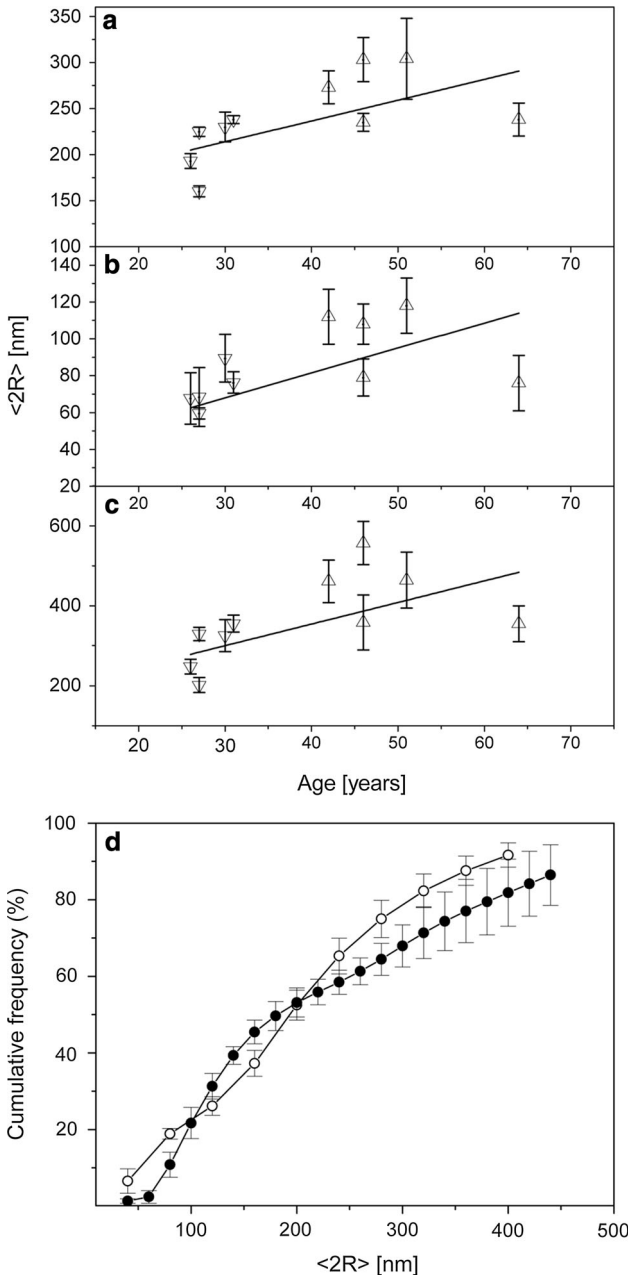

Fig. 3 Semen prostasomes average size as a function of the donor age. Panel **a** average hydrodynamic diameter of prostasomes obtained from the cumulant analysis, which does not distinguish different subpopulations: *empty down triangle* "young donors" and *empty up triangle* "elder donors." In panel **b** and **c,** the peak values of the two subpopulations are shown, which can be resolved by analyzing the correlation function using the exponential sampling algorithm. *Curves* are linear fits on both the young and elder groups. **d** Cumulative size distribution averaged on the elder (*empty circles*) and young (*filled circles*) donor groups. Also in terms of cumulative distribution, although the individual variation contribute non-negligible uncertainties, there is a significant prevalence of the larger vesicles in the elder donors

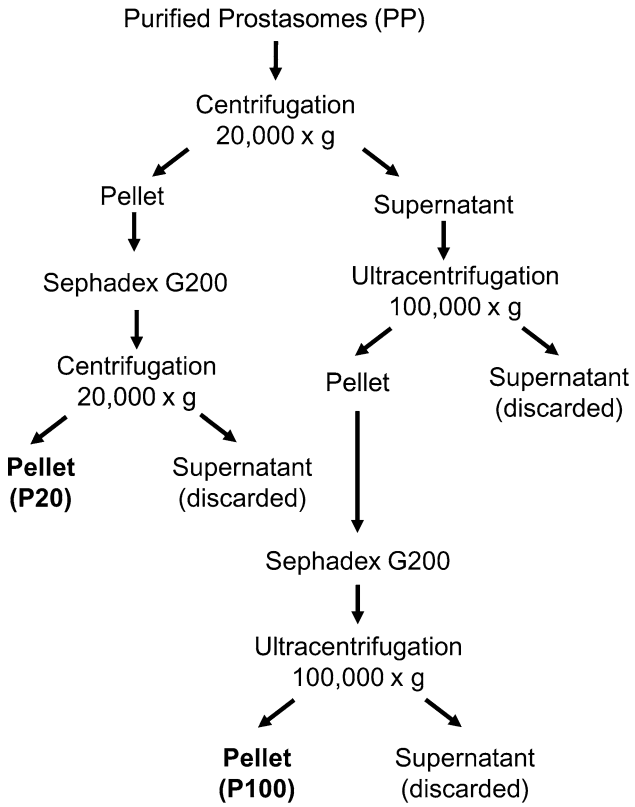

Fig. 4 Experimental scheme for the isolation of the two different prostasome populations

resuspended in 2 mL of 30 mM Tris, 130 mM NaCl, pH 7.4, and purified in Sephadex G200 to remove contaminants. Eluates from gel filtration were centrifuged at $20{,}000\times g$ and $100{,}000\times g$, resuspended in the same Tris buffer and named, respectively, P20 and P100 fractions. Prostasomes recovered by preparative ultracentrifugation from human seminal fluid of single donors were isolated following the same protocol, without performing size-exclusion chromatography. Aliquots of the fractions isolated from P20 and P100 pools and individual donors were then checked by DLS to ensure the enrichment of the prostasomes .

Lipid Composition of the Different Prostasome Populations

To investigate the lipid composition of the two populations of prostasomes, we compared the distribution between the different lipid classes in the P20 and P100 fractions isolated from pooled samples of seminal plasma ($n = 20$). Results are reported in Table 1. The most noticeable dif-

Table 1 Quantification of lipid content in the two prostasome populations

Lipids	P100 (80 nm)	P20 (300 nm)
Cholesterol[a]	0.85 ± 0.2	0.98 ± 0.4
Total lipid phosphorus	0.44 ± 0.1	0.54 ± 0.3
Cholesterol/phospholipid ratio	1.93	1.81
Phosphatidylethanolamine[b]	15 ± 4	16 ± 4
Phosphatidylcholine[b]	12 ± 3	13 ± 1
Sphingomyelin[b]	53 ± 12	57 ± 11
Phosphatidylserine[b]	13 ± 3	9 ± 2
Phosphatidylinositol[b]	7 ± 3	5 ± 1

The reported results are the average of five determinations

[a] Results expressed as μmol/mg-1 protein ± SEM

[b] Results expressed as percentage of total lipid phosphorus in each phospholipid class ±SEM

ference was the molar ratio cholesterol/phospholipids 1.93–1.81, which emphasizes the peculiarities of these fractions when compared to the usual ratio present in plasma membranes. In addition, sphingomyelin was plentiful, where partially substituted phosphatidylethanolamine and phosphatidylcholine were less abundant. These results obtained in both the populations have substantially confirmed previous reports (Arienti et al. 1998; Arvidson et al. 1989).

Aminopeptidase Activity

We tested the aminopeptidase activity of the two vesicle populations to verify if this enzyme, initially reported as a marker of prostasomes (Arienti et al. 1997b), was present in both vesicle types. Suc(Ala)3pNA was used as the substrate for activity determination. Both populations of prostasomes were able to hydrolyze the substrate with a Vmax of 4.0–4.7 mmol mg prot-1 h-1 and a Km of 0.38–0.45 mM. The addition of 1 % Thesit to the incubation mixture was without effects in both samples, thus excluding the possibility of latency. Optimal pH was about 7.5, and the activity was stable after freezing and thawing but was destroyed upon heating at 65 °C for 10 min. These findings substantially confirmed a previous report (Arienti et al. 1997b).

A number of substances (EDTA, up to 10 mmol/L, iodoacetamide from 0.16 to 1.35 mmol/L, benzamidine 0.11–0.9 mmol/L and diisopropylfluorophosphate from 0.11 to 0.90 mmol/L) were without effect on enzyme activity. All together, these data indicate that the enzyme, in both the populations of prostasomes, was a serine protease-dependent and Zn^{2+} for activity, and that this activity is the same as described by Lilja and Laurel (Lilja and Laurell 1984).

Proteomic Analysis of Prostasomes Isolated from Human Semen

Two different experimental set-ups were performed. First, we analyzed prostasomes fractions (P100 and P20) isolated from pooled samples of human semen ($n = 20$). For this analysis, the samples were initially pooled and then subjected to isolation. For each fraction, 5 technical replicates were produced for a total of 10 gels included in the first matching. The second analysis involved prostasomes fractions (P100 and P20) isolated from the two groups of subjects and analyzed by 2-DE with a single technical replicate. The two experimental set-ups were also matched against each other to verify the trend in single patients of the differentially expressed proteins between the two fractions. In the pooled analysis, the average number of matched polypeptide spots in all the 2-DE gels from the two experimental groups was 342 ± 6. The coefficient of variation (CV) of the individual spot volumes was 32 % in P20 group, while it was 34 % in P100 group, showing a technical variability in line with previous data (Molloy et al. 2003). Representative gel images are reported in supplementary Fig. 1. The 2-DE analysis of the pooled semen samples found, in total, 42 differentially expressed polypeptides spots according to our statistical framework. Of these, 20 polypeptide spots were up-regulated in the P100 fraction, while 22 were decreased in the P100 with respect to the P20 fraction. Using LC–MS/MS, we were able to identify 25 out of 42 of the differentially expressed spots, while for the remaining 17 spots, we could not obtain significant hits in the database search (Fig. 5a). Table 2 shows the differentially expressed polypeptide spots identified in the P100 and P20 fractions of the pooled analysis. GO analysis of up-regulated proteins in the P100 fraction showed an enrichment in biological processes related to virus-host interaction and endosomal sorting of proteins, while the prominent molecular functions were related to calcium binding and peptidase activities. Interestingly, most of the up-regulated proteins in the P100 population showed association with terms related to vesicles, especially to late endosomal sorting (supplementary Table 1). On the other hand, proteins increased in the P20 fraction were enriched in different processes and functions. The major biological processes involved were related to proteolysis, protein degradation, and antigen processing, while the enriched molecular functions were linked to ubiquitin binding and peptidase activity (supplementary Table 1). Notably, the enriched cellular compartment terms for the P20 population were the proteasome complex and the cytosol. Major differences in protein expression were noticed for the expression of three proteins involved in exosome biogenesis and vesicle trafficking (Baietti et al. 2012), the programmed cell death 6-interacting protein

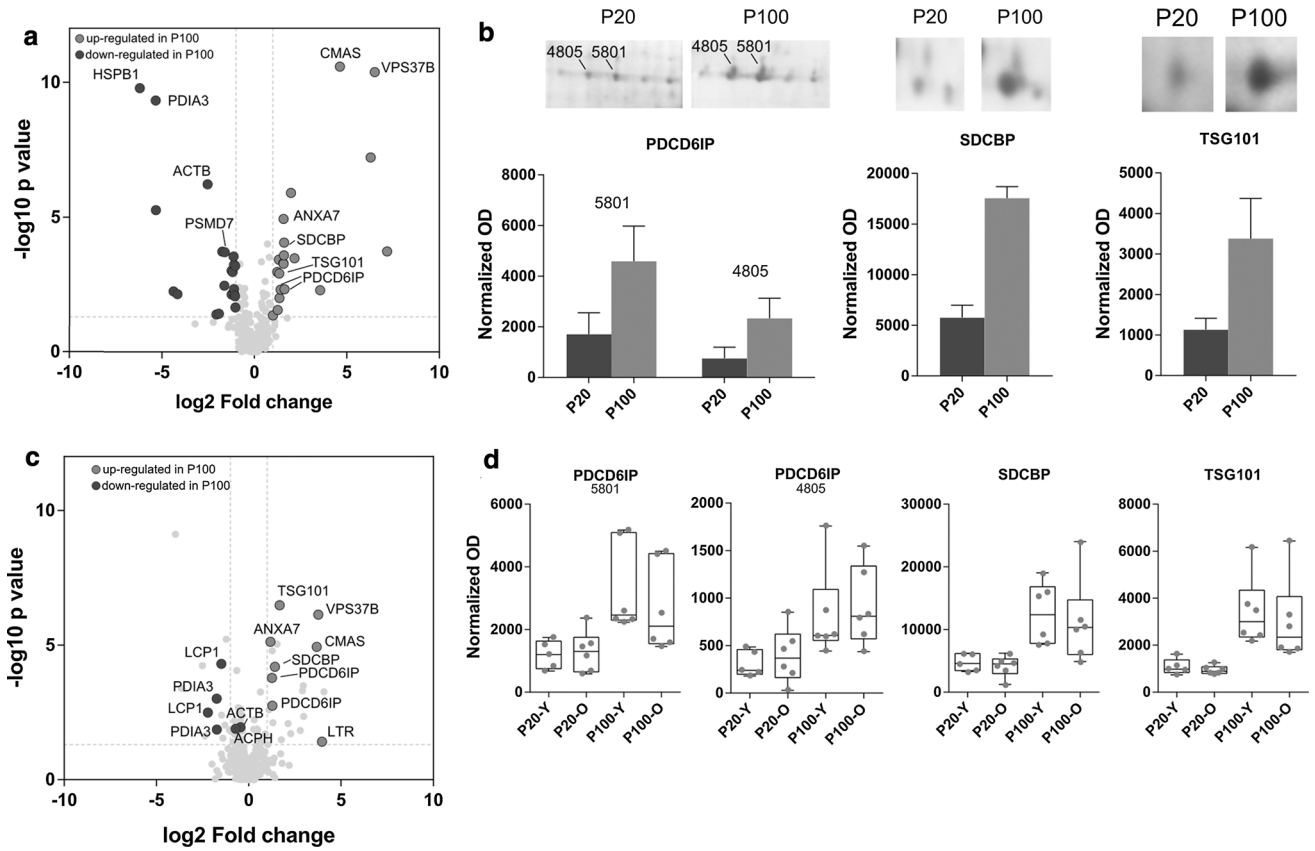

Fig. 5 Differential protein expression in the two EV populations isolated from human semen. **a** Volcano plot of the protein expression levels in the pooled analysis. **b** Enrichment of exosomal markers in the P100 population. **c** Volcano plot of the protein expression levels in the single subject analysis. Labeled proteins (Gene name) were significantly differentially expressed. **d** *Box plot* of the three exosomal marker across the young (Y)/elder (O) subjects and the two EV populations (P100 and P20)

(PDCD6IP also called alix), tumor susceptibility gene 101 protein (TSG101, fold change 2.98), and syntenin-1 (SDCBP, fold change 3.05, Fig. 5b). PDCD6IP was identified in two different spots, with a fold change of 2.68 and 3.09. These spots are presumably the phosphorylated forms of PDCD6IP, as several phosphosites are known for this protein (Olsen et al. 2010). Anyway, no phosphopeptides were detected by MS (data not shown). The highest fold changes were found for the *N*-acylneuraminate cytidylyltransferase (CMAS) and the vacuolar protein sorting-associated protein 37B (VPS37B; $+\infty$ not present in the P20 fraction). Among the down-regulated proteins in the P100 population, the highest fold changes ($-\infty$, not present in P100) were found for a spot for which it was not possible to obtain a unique identification and containing two proteins, the protein disulfide-isomerase A3 (PDIA3) and cytosolic non-specific peptidase 2 (CDNP2). Another spot showing strong down-regulation in the P100 population was identified as the heat shock protein beta-1 (HSPB1).

To evaluate in silico the modality of secretion of the differentially expressed proteins in the two subpopulations of prostasomes, we used the webserver SecretomeP. Only four proteins had a signal peptide for classical secretion, while 9 out of 22 showed positive association with unconventional secretion. The remaining 8 proteins did not have a positive score for unconventional secretion, so according at least to the protein sequence, they are believed to mainly localize inside the cell (supplementary Fig. 2). To validate the differential expression of the identified proteins for the two prostasome populations, we performed a 2-DE analysis of semen vesicles isolated from individual subjects within two different age ranges <35 (defined as young, 28.8 ± 2.6 years, $n = 6$) and >35 years (defined as elder, 50.2 ± 7.7 years, $n = 6$), using the same methods. The average number of matched polypeptide spots in the single subject analysis was similar to the pooled one, 302 ± 26. As expected, the variability of the quantification in the single subject analysis was much higher that in the pooled analysis. The average CV of individual spot volumes was 66 % in P20 group while it was 68 % in P100 group. This was possibly due to the cumulative effect of technical and biological variability. Out of the 26 polypeptide spots identified in the pooled analysis, 14 were also differentially expressed in the single subject analysis

Table 2 Differentially expressed polypeptide spots in the two prostasomes populations of the pooled analysis

ID spot	Gene name	Uniprot Accession	Protein name	# identified peptides	Sequence coverage (%)	MASCOT score	MW (KDa) theor./exp.	pI Theor./exp.	Pooled analysis	
									Fold change P100 vs P20	*p* value P100 vs P20
7409	CMAS	NEUA_HUMAN	*N*-acylneuraminate cytidylyltransferase	2	1	44	48.4/50.0	8.16/7.25	$+\infty$	2.62E−11
6209	VPS37B	VP37B_HUMAN	Vacuolar protein sorting-associated protein 37B	1	3	48	31.3/37.2	6.78/6.80	$+\infty$	4.19E−11
8101	SDCBP	SDCB1_HUMAN	Syntenin-1	5	21	111	32.4/32.0	7.06/7.46	3.04	8.84E−05
7010	TMPS2	TMPS2_HUMAN	Transmembrane protease serine 2	1	2	65	53.9/26.0	8.12/7.50	3.02	2.62E−04
4411	ANXA7	ANXA7_HUMAN	Annexin A7	7	13	206	52.7/45.0	5.52/6.20	2.99	1.16E−05
4405	TSG101	TS101_HUMAN	Tumor susceptibility gene 101 protein	5	12	85	43.9/49.0	6.06/6.12	2.98	5.35E−04
8503	ANXA11	ANX11_HUMAN	Annexin A11	3	7	120	54.4/55.0	7.53/7.60	2.95	5.11E−04
5801	PDCD6IP	PDC6I_HUMAN	Programmed cell death 6-interacting protein	16	20	372	96.0/100.0	6.13/6.43	2.68	4.84E−03
4805	PDCD6IP	PDC6I_HUMAN	Programmed cell death 6-interacting protein	2	2	40	96.0/100.0	6.13/6.10	3.09	4.74E−03
0006	GGT1	GGT1_HUMAN	Gamma-glutamyltranspeptidase 1	1	2	110	61.4/25.0	6.65/5.30	2.54	1.23E−03
3803	LTR	TRFL_HUMAN	Lactotransferrin	4	6	115	78.2/87.0	8.50/6.02	2.40	2.79E−02
1202	CKB	KCRB_HUMAN	Creatine kinase B-type	3	10	129	42.6/41.0	5.34/5.52	−2.04	2.24E−02
3502	PDIA3	PDIA3_HUMAN	Protein disulfide-isomerase A3	2	4	46	56.8/59.0	5.98/5.90	−2.06	8.66E−03
1801	VCP	TERA_HUMAN	Transitional endoplasmic reticulum ATPase	8	11	256	89.3/105.0	5.14/5.32	−2.14	5.79E−04
3203	PSMD13	PSD13_HUMAN	26S proteasome non-ATPase regulatory subunit 13	6	21	217	42.9/42.0	5.53/5.92	−2.15	4.62E−03
1602	LCP1	PLSL_HUMAN	Plastin-2	11	22	307	70.3/71.0	5.29/5.30	−3.07	3.49E−03
1608	LCP1	PLSL_HUMAN	Plastin-2	4	7	152	70.3/71.0	5.29/5.50	−3.04	2.01E−04
1613	LCP	PLSL_HUMAN	Plastin-2	1	1	44	70.3/71.0	5.29/5.40	−2.56	9.69E−02
2005	APCS	SAMP_HUMAN	Serum amyloid P-component	15	3	97	25.5/27.0	6.10/5.75	−2.18	2.87E−04
5605	STIP1	STIP1_HUMAN	Stress-induced-phosphoprotein 1	1	1	62	63.2/70.0	6.40/6.63	−2.20	6.54E−03
1706	APEH	ACPH_HUMAN	Acylamino-acid-releasing enzyme	3	6	127	82.1/90.0	5.29/5.50	−2.26	1.09E−03
7203	PSDM7	PSD7_HUMAN	26S proteasome non-ATPase regulatory subunit 7	1	3	59	37.1/38.0	6.29/7.11	−3.33	1.91E−04
3304	ACTB	ACTB_HUMAN	Actin, cytoplasmic 1	4	13	93	42.1/43.0	5.29/5.98	−5.79	6.10E−07
2505	CNDP2	CNDP2_HUMAN	Cytosolic non-specific dipeptidase	2	6	76	52.9/56.9	5.65/5.87	$-\infty$	4.72E−10
	PDAI3	PDIA3_HUMAN	Protein disulfide-isomerase A3	1	1	50	56.8/56.9	5.98/5.87	$-\infty$	4.72E−10

Table 2 continued

ID spot	Gene name	Uniprot Accession	Protein name	# identified peptides	Sequence coverage (%)	MASCOT score	MW (KDa) theor./exp.	pI Theor./exp.	Pooled analysis	
									Fold change P100 vs P20	p value P100 vs P20
3008	HSPB1	HSPB1_HUMAN	Heat shock protein beta-1	1	8	51	22.8/26.0	5.98/5.90	$-\infty$	1.64E−10

Spot ID, gene name, Uniprot accession, protein name, number of identified peptides, Mascot score, theoretical and experimental molecular weight (MW), and isoelectric point are reported in the table. Fold changes (FC) and p value according to student test are also reported. Fold changes are calculated against P100 population

between the P100 and P20 vesicle populations (highlighted in Fig. 5c). Up-regulation in the P100 population was confirmed for 8 polypeptide spots, including TSG101, PDCD6IP, SDCBP and VPS37B. Down-regulation was confirmed for two spots containing plastin-2 (LCP1) and for the two spots containing PDIA3, while the acylamino-acid-releasing enzyme (APEH) and the actin 1 (ACTB) were significantly down-regulated but with a fold change <2. Notably, the CVs for the normalized optical density of the three endosomal sorting complexes required for transport (ESCRT) proteins TSG101, PDCD6IP, and SDCBP were ranging between 29 % and 73 %, highlighting a high contribution of biological variability for the levels of these three proteins, especially in the P100 population. No significant differences were noticed for these three proteins in the comparison between the young and elderly groups (Fig. 5d).

Discussion

Here we characterized by means of robust biophysical and biochemical methods two distinct populations of prostasomes present in human seminal fluid. Based on our results, we could clearly distinguish a smaller (P100, hydrodynamic radius ≈ 80 nm) and a larger subpopulations (P20, hydrodynamic radius ≈ 300 nm) of vesicles. These two populations were isolated at different centrifugation speed and were also characterized by enrichment in specific protein markers. Notably, the two prostasomes populations had a peculiar phospholipid composition, a high amount of cholesterol and expressed aminopeptidase activity. These peculiarities detected in both the populations were already shown in previous reports. EVs isolated from human semen have been historically called as prostasomes (Raposo and Stoorvogel 2013). In particular, the prostasomes are thought to be the storage vesicles of prostate epithelial cells (Sahlen et al. 2002). Earlier studies had already shown the heterogeneity and/or the different subpopulations of vesicles in human semen (Bordi et al. 2001; Stridsberg et al. 1996). More recently, Aalberts and colleagues have shown two distinct subpopulations of prostasomes isolated from vasectomized men, one with a diameter of 50 nm and one with a larger diameter (100 nm), having a similar floating density in sucrose gradients (Aalberts et al. 2012). Other studies used nanoparticle tracking methods to show an average diameter size of prostasomes between 30 and 200 nm (Ronquist 2012). In our study, we used DLS to measure size and size distribution of particles in native conditions, obtaining a different average diameter of the two populations isolated with differential centrifugation. This may depend from several factors. Some previous studies were performed on

semen isolated from vasectomized men, possibly excluding the vesicles derived from epididymis. Here the population of vesicles might be mixed and derived from different organs, such as prostate, epididymis, or accessory glands. For instance, PDIA3, a marker of the vesicles isolated after 20,000×*g* centrifugation is a protein constitutively expressed in the epididymal structures (Akama et al. 2010). However, no specific tissue marker characterized the two prostasome populations. Another explanation might be related to DLS properties. The majority of the studies on prostasomes and EV have been performed with electron microscopy which has harsh condition of fixing and limited sampling power, because only few vesicles can be reliably measured in each microscopy field. The statistical framework and native conditions of DLS may give a different estimation of the average size distribution of prostasomes. The size distribution was also influenced by other factors such as pH and albumin. Albumin is a cholesterol acceptor and the binding of this protein to vesicles may increase their apparent size, indeed, about 25 % of the albumin added to the suspension was bound to the vesicles.

The lipid composition of the two prostasome populations isolated in this work was similar to previous studies, confirming the peculiar membrane composition of these vesicles and the high cholesterol/phospholipid ratio (~2) (Arienti et al. 1998). However, we did not notice any significant difference between the two prostasome populations in lipid composition as shown in previous reports. Brouwers and colleagues found a higher content of sphingomyelin in the population with a larger diameter (100 nm), while the total content of hexosylceramide was higher in the smaller population (Brouwers et al. 2013). Yet the total percentage of the different phospholipid classes was not substantially different between the two prostasome populations, as in our results.

The heterogeneity of the isolated prostasomes could also be seen at the protein level and among individual patients. For instance, the proteins TSG101 and PDCD6IP are often used as markers for exosome isolation and also as normalization factor when analyzing protein expression. It has already been shown a high inter-patient variability of these markers in vesicles isolated from blood (Bastos-Amador et al. 2012); thus care should be taken when reporting results of protein expression using these proteins as normalization factor. Here, using 2-DE, we noticed a high inter-patient variability especially in the prostasome population isolated using 100,000×*g*, thereby confirming the previous results also in EVs isolated from semen.

The two prostasomes populations had only a partially different 2-DE pattern, but some polypeptide spots were differentially expressed either in the P20 or P100 populations. Interestingly, we noticed a significant enrichment of proteins involved in endosomal sorting and exosomes biogenesis, such as alix, TSG101, and syntenin-1 in the smaller prostasomes (Baietti et al. 2012). This is also confirmed by the presence of the protein VPS37B, which is a core component of the ESCRT-I protein complex together with TSG101 (Stuchell et al. 2004). Therefore, centrifugation at 100,000×*g* may enrich in smaller vesicles mostly originating from multivesicular bodies and secreted via an ESCRT-I-dependent mechanism. The presence of the same proteins in the larger population may indicate similar trafficking pathways or may be technical, due to the relatively low resolution power of step-wise differential centrifugation (Bobrie et al. 2012).

Prostasome can deliver lipids, proteins, and ions to spermatozoa upon fusion and/or interaction (Arienti et al. 1997a). This transfer can modulate directly or indirectly processes like fertilization and capacitation (Palmerini et al. 2003). For instance, we found that CMAS, a protein involved in sialylation, was identified only in the P100 population. Notably, sialylation is a fundamental process during sperm capacitation (Ma et al. 2012). CMAS produces the activated cytidine 5′-monophosphate *N*-acetylneuraminic acid (CMP-NeuNAc), a necessary substrate for sialyltransferases. Therefore, it is possible that the prostasome-mediated transfer of CMAS to sperm cells may contribute to the regulation of the CMP-NeuNAc levels, influencing global sialylation of sperm cells proteins. An increase in protein sialylation may in turn contribute to the proposed inhibitory role of prostasome in sperm capacitation, which is dependent also from their high content in cholesterol (Pons-Rejraji et al. 2011).

Notably, the transmembrane protease serine 2 (TMPRSS2) was also over-expressed in the P100 prostasomes. This protein is highly expressed in prostate tissue and is an androgen-regulated gene (Lin et al. 1999). Chromosomal rearrangements leading to fusions of TMPRSS2 to the oncogenic transcription factor ERG occur in prostate cancers (Clark et al. 2007). The fusion product TMPRSS2:ERG is actively investigated as prostate cancer biomarker (Lin et al. 2013) and the detection of TMPRSS2 in biological fluids may be further exploited as a biomarker for prostate cancer, considering that this protein has already been identified in exosomes from different biofluids, including urine (Gonzales et al. 2009). On the other hand, we found that larger vesicles pelleting at 20,000×*g* were characterized by the presence of the transitional endoplasmic reticulum ATPase (VCP). This protein has an ATPase activity and possesses an array of different functions, mainly related to protein degradation (Yamanaka et al. 2012). Notably, VCP has been linked to the process of sperm capacitation, being among the proteins which are phosphorylated upon the beginning of capacitation (Ficarro et al. 2003). Moreover, VCP has also been proposed as a poor prognosis biomarker for prostate cancer (Tsujimoto et al. 2004).

The differential protein expression found in the two subpopulations of prostasomes substantiates the notion of different roles of the semen vesicles toward the target cells, and/or distinct secretion pathways from the organ of origin. Furthermore, the presence in prostasomes of proteins whose expression is abundant in the prostate or which have been implicated in prostate cancer may support the biomarker potential of these vesicles.

Acknowledgments This work was funded by Fondazione Cassa di Risparmio di Perugia (Grant Number 2010.011.0396).

Conflicts of interest The authors declare that there are no conflicts of interest.

References

Aalberts M, van Dissel-Emiliani FM, van Adrichem NP, van Wijnen M, Wauben MH, Stout TA, Stoorvogel W (2012) Identification of distinct populations of prostasomes that differentially express prostate stem cell antigen, annexin A1, and GLIPR2 in humans. Biol Reprod 86:82

Akama K, Horikoshi T, Sugiyama A, Nakahata S, Akitsu A, Niwa N, Intoh A, Kakui Y, Sugaya M, Takei K, Imaizumi N, Sato T, Matsumoto R, Iwahashi H, Kashiwabara S, Baba T, Nakamura M, Toda T (2010) Protein disulfide isomerase-P5, down-regulated in the final stage of boar epididymal sperm maturation, catalyzes disulfide formation to inhibit protein function in oxidative refolding of reduced denatured lysozyme. Biochim Biophys Acta 1804:1272–1284

Arienti G, Carlini E, Palmerini CA (1997a) Fusion of human sperm to prostasomes at acidic pH. J Membr Biol 155:89–94

Arienti G, Carlini E, Verdacchi R, Palmerini CA (1997b) Transfer of aminopeptidase activity from prostasomes to sperm. Biochim Biophys Acta 1336:269–274

Arienti G, Carlini E, Polci A, Cosmi EV, Palmerini CA (1998) Fatty acid pattern of human prostasome lipid. Arch Biochem Biophys 358:391–395

Arvidson G, Ronquist G, Wikander G, Ojteg AC (1989) Human prostasome membranes exhibit very high cholesterol/phospholipid ratios yielding high molecular ordering. Biochim Biophys Acta 984:167–173

Baietti MF, Zhang Z, Mortier E, Melchior A, Degeest G, Geeraerts A, Ivarsson Y, Depoortere F, Coomans C, Vermeiren E, Zimmermann P, David G (2012) Syndecan-syntenin-ALIX regulates the biogenesis of exosomes. Nat Cell Biol 14:677–685

Bartlett GR (1959) Colorimetric assay methods for free and phosphorylated glyceric acids. J Biol Chem 234:469–471

Bastos-Amador P, Royo F, Gonzalez E, Conde-Vancells J, Palomo-Diez L, Borras FE, Falcon-Perez JM (2012) Proteomic analysis of microvesicles from plasma of healthy donors reveals high individual variability. J Proteomics 75:3574–3584

Bendtsen JD, Jensen LJ, Blom N, Von Heijne G, Brunak S (2004) Feature-based prediction of non-classical and leaderless protein secretion. Protein Eng Des Sel 17:349–356

Berne BJ, Pecora R (1976) Dynamic light scattering: with applications to chemistry, biology, and physics. Dover, New York

Bobrie A, Colombo M, Krumeich S, Raposo G, Thery C (2012) Diverse subpopulations of vesicles secreted by different intracellular mechanisms are present in exosome preparations obtained by differential ultracentrifugation. J Extracell Vesicles. doi:10.3402/jev.v1i0.18397

Bordi F, Cametti C, De Luca F, Carlini E, Palmerini CA, Arienti G (2001) Hydrodynamic radii and lipid transfer in prostasome self-fusion. Arch Biochem Biophys 396:10–15

Brouwers JF, Aalberts M, Jansen JW, van Niel G, Wauben MH, Stout TA, Helms JB, Stoorvogel W (2013) Distinct lipid compositions of two types of human prostasomes. Proteomics 13:1660–1666

Chiasserini D, Tozzi A, de Iure A, Tantucci M, Susta F, Orvietani PL, Koya K, Binaglia L, Calabresi P (2011) Mortalin inhibition in experimental Parkinson's disease. Mov Disord 26:1639–1647

Clark J, Merson S, Jhavar S, Flohr P, Edwards S, Foster CS, Eeles R, Martin FL, Phillips DH, Crundwell M, Christmas T, Thompson A, Fisher C, Kovacs G, Cooper CS (2007) Diversity of TMPRSS2-ERG fusion transcripts in the human prostate. Oncogene 26:2667–2673

Fabiani R (1994) Functional and biochemical characteristics of human prostasomes. Minireview based on a doctoral thesis. Upsala J Med Sci 99:73–111

Ficarro S, Chertihin O, Westbrook VA, White F, Jayes F, Kalab P, Marto JA, Shabanowitz J, Herr JC, Hunt DF, Visconti PE (2003) Phosphoproteome analysis of capacitated human sperm. Evidence of tyrosine phosphorylation of a kinase-anchoring protein 3 and valosin-containing protein/p97 during capacitation. J Biol Chem 278:11579–11589

Folch J, Lees M, Sloane Stanley GH (1957) A simple method for the isolation and purification of total lipides from animal tissues. J Biol Chem 226:497–509

Gonzales PA, Pisitkun T, Hoffert JD, Tchapyjnikov D, Star RA, Kleta R, Wang NS, Knepper MA (2009) Large-scale proteomics and phosphoproteomics of urinary exosomes. J Am Soc Nephrol 20:363–379

Goormaghtigh E, Scarborough GA (1986) Density-based separation of liposomes by glycerol gradient centrifugation. Anal Biochem 159:122–131

Greenwood AI, Tristram-Nagle S, Nagle JF (2006) Partial molecular volumes of lipids and cholesterol. Chem Phys Lipids 143:1–10

Haridas MM, Bellare JR (1998) Differences in particle sizes measured by cryo-SEM and quasi-elastic light-scattering in latex-particles. Colloids Surf A 133:165–171

Jin L, Yu YX, Gao GH (2006) A molecular-thermodynamic model for the interactions between globular proteins in aqueous solutions: applications to bovine serum albumin (BSA), lysozyme, alpha-chymotrypsin, and immuno-gamma-globulins (IgG) solutions. J Colloid Interface Sci 304:77–83

Juyena NS, Stelletta C (2012) Seminal plasma: an essential attribute to spermatozoa. J Androl 33:536–551

Kelly RW (1995) Immunosuppressive mechanisms in semen: implications for contraception. Hum Reprod 10:1686–1693

Kelly RW, Holland P, Skibinski G, Harrison C, McMillan L, Hargreave T, James K (1991) Extracellular organelles (prostasomes) are immunosuppressive components of human semen. Clin Exp Immunol 86:550–556

Lilja H, Laurell CB (1984) Liquefaction of coagulated human semen. Scand J Clin Lab Invest 44:447–452

Lilja H, Weiber H (1983) Gamma-Glutamyl transferase bound to prostatic subcellular organelles and in free form in human seminal plasma. Scand J Clin Lab Invest 43:307–312

Lin B, Ferguson C, White JT, Wang S, Vessella R, True LD, Hood L, Nelson PS (1999) Prostate-localized and androgen-regulated expression of the membrane-bound serine protease TMPRSS2. Cancer Res 59:4180–4184

Lin DW, Newcomb LF, Brown EC, Brooks JD, Carroll PR, Feng Z, Gleave ME, Lance RS, Sanda MG, Thompson IM, Wei JT, Nelson PS, Canary Prostate Active Surveillance Study I (2013) Urinary TMPRSS2:ERG and PCA3 in an active surveillance cohort: results from a baseline analysis in the Canary Prostate Active Surveillance Study. Clin Cancer Res 19:2442–2450

Ma F, Wu D, Deng L, Secrest P, Zhao J, Varki N, Lindheim S, Gagneux P (2012) Sialidases on mammalian sperm mediate deciduous sialylation during capacitation. J Biol Chem 287: 38073–38079

Mann T, Lutwak-Mann C (1981) Male reproductive function and semen. Springer, Berlin

Molloy MP, Brzezinski EE, Hang J, McDowell MT, VanBogelen RA (2003) Overcoming technical variation and biological variation in quantitative proteomics. Proteomics 3:1912–1919

Monkos K (1996) Viscosity of bovine serum albumin aqueous solutions as a function of temperature and concentration. Int J Biol Macromol 18:61–68

Nakamura K, Handa S (1984) Coomassie brilliant blue staining of lipids on thin-layer plates. Anal Biochem 142:406–410

Olsen JV, Vermeulen M, Santamaria A, Kumar C, Miller ML, Jensen LJ, Gnad F, Cox J, Jensen TS, Nigg EA, Brunak S, Mann M (2010) Quantitative phosphoproteomics reveals widespread full phosphorylation site occupancy during mitosis. Sci Signal 3:ra3

Olsson I, Ronquist G (1990) Isoenzyme pattern of lactate dehydrogenase associated with human prostasomes. Urol Int 45:346–349

Palmerini CA, Saccardi C, Carlini E, Fabiani R, Arienti G (2003) Fusion of prostasomes to human spermatozoa stimulates the acrosome reaction. Fertil Steril 80:1181–1184

Pons-Rejraji H, Artonne C, Sion B, Brugnon F, Canis M, Janny L, Grizard G (2011) Prostasomes: inhibitors of capacitation and modulators of cellular signalling in human sperm. Int J Androl 34:568–580

Raposo G, Stoorvogel W (2013) Extracellular vesicles: exosomes, microvesicles, and friends. J Cell Biol 200:373–383

Ronquist G (1987) Effect of modulators on prostasome membrane-bound ATPase in human seminal plasma. Eur J Clin Invest 17:231–236

Ronquist G (2012) Prostasomes are mediators of intercellular communication: from basic research to clinical implications. J Intern Med 271:400–413

Ronquist G, Frithz GG (1986) Prostasomes in human semen contain ADP and GDP. Acta Eur Fertil 17:273–276

Ronquist GK, Larsson A, Stavreus-Evers A, Ronquist G (2012) Prostasomes are heterogeneous regarding size and appearance but affiliated to one DNA-containing exosome family. Prostate 72:1736–1745

Rooney IA, Atkinson JP, Krul ES, Schonfeld G, Polakoski K, Saffitz JE, Morgan BP (1993) Physiologic relevance of the membrane attack complex inhibitory protein CD59 in human seminal plasma: CD59 is present on extracellular organelles (prostasomes), binds cell membranes, and inhibits complement-mediated lysis. J Exp Med 177:1409–1420

Sahlen GE, Egevad L, Ahlander A, Norlen BJ, Ronquist G, Nilsson BO (2002) Ultrastructure of the secretion of prostasomes from benign and malignant epithelial cells in the prostate. Prostate 53:192–199

Stegmayr B, Ronquist G (1982) Promotive effect on human sperm progressive motility by prostasomes. Urol Res 10:253–257

Stepanek P (1993) Data analysis in dynamic light scattering. Oxford University Press, Oxford

Stridsberg M, Fabiani R, Lukinius A, Ronquist G (1996) Prostasomes are neuroendocrine-like vesicles in human semen. Prostate 29:287–295

Stuchell MD, Garrus JE, Muller B, Stray KM, Ghaffarian S, McKinnon R, Krausslich HG, Morham SG, Sundquist WI (2004) The human endosomal sorting complex required for transport (ESCRT-I) and its role in HIV-1 budding. J Biol Chem 279:36059–36071

Susta F, Chiasserini D, Fettucciari K, Orvietani PL, Quotadamo F, Noce R, Bartoli A, Marconi P, Corazzi L, Binaglia L (2010) Protein expression changes induced in murine peritoneal macrophages by Group B Streptococcus. Proteomics 10: 2099–2112

Tsujimoto Y, Tomita Y, Hoshida Y, Kono T, Oka T, Yamamoto S, Nonomura N, Okuyama A, Aozasa K (2004) Elevated expression of valosin-containing protein (p97) is associated with poor prognosis of prostate cancer. Clin Cancer Res 10:3007–3012

Vilker VL, Dileo AJ, Colton CK, Smith KA (1979) Device for the measurement of small liquid flow rates. Rev Sci Instrum 50:640

Wang J, Duncan D, Shi Z, Zhang B (2013) WEB-based GEne SeT analysis toolkit (WebGestalt): update 2013. Nucleic Acids Res 41:W77–W83

Wilson MJ, Steer RC, Kaye KW (1984) Protein kinase activities in human prostatic secretion: biochemical characterization and effect of prostatitis. J Lab Clin Med 103:905–911

Yadav S, Shire SJ, Kalonia DS (2011) Viscosity analysis of high concentration bovine serum albumin aqueous solutions. Pharm Res 28:1973–1983

Yamanaka K, Sasagawa Y, Ogura T (2012) Recent advances in p97/VCP/Cdc48 cellular functions. Biochim Biophys Acta 1823:130–137